Supplement of

Reactive nitrogen in and around the northeastern and Mid-Atlantic US: sources, sinks, and connections with ozone

Huang et al.

Correspondence to: Min Huang (minhuang@umd.edu)

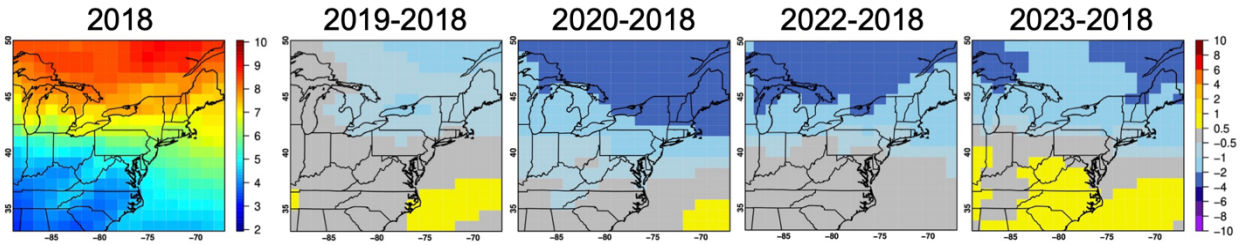

Figure S1: Stratospheric influences on MJJ surface-level O_3 and their interannual differences (all in ppbv), based on WRF-Chem's chemical boundary condition models' stratospheric O_3 tracer.

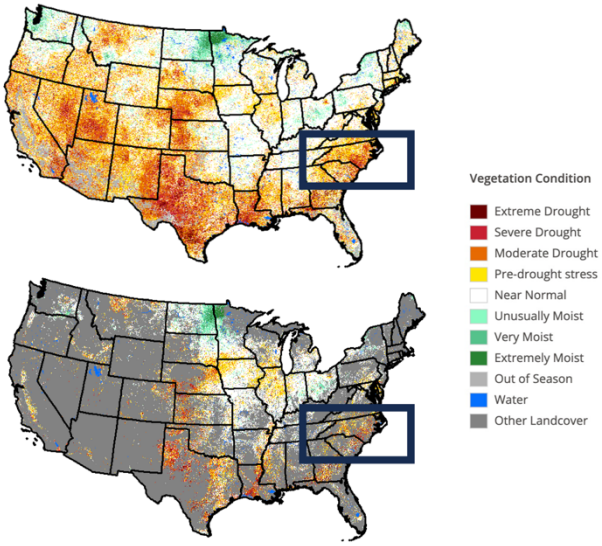

Figure S2: Vegetation Drought Response Index (VegDRI, retrieved from https://vegdri.unl.edu), at 1 km^2 spatial resolution for the week of 20–26 June 2022, for (upper) all land cover types and (lower) croplands only. Conditions for the following week look similar. The development of VegDRI involves satellite observations of vegetation types and conditions, as well as soil characteristics and climate data. The focused area in the irrigation case study is indicated by dark-blue boxes in both panels.

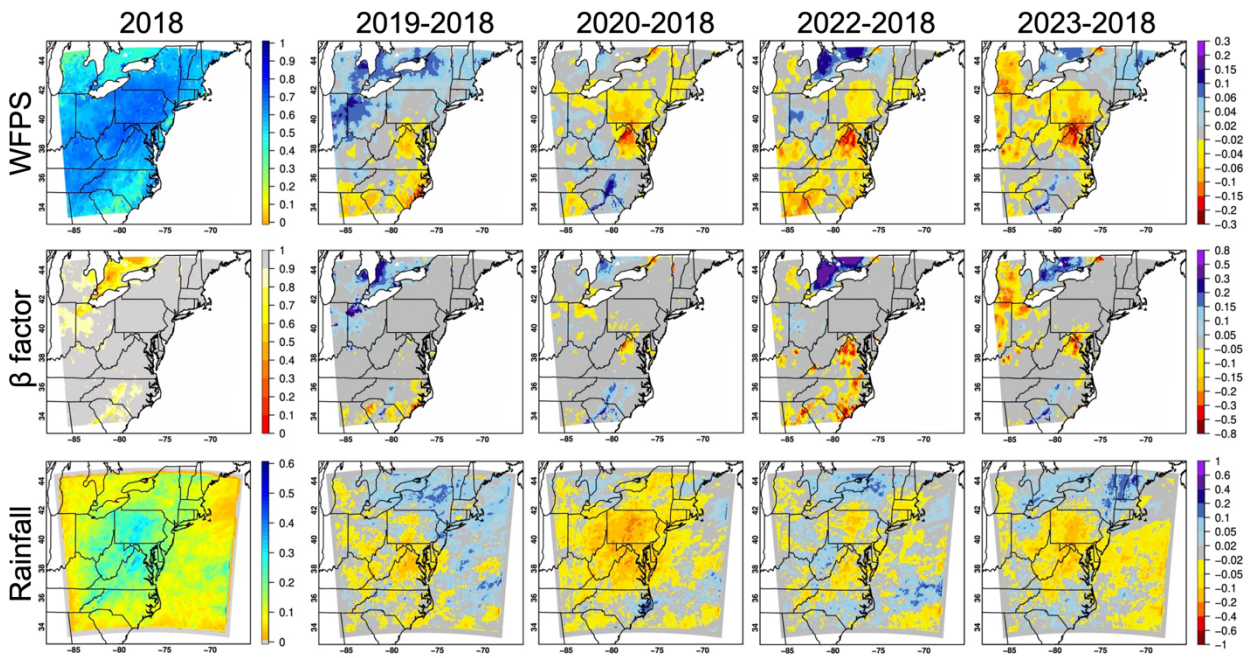

Figure S3: MJJ (upper) water-filled pore space θ; (middle) daytime SM factor controlling stomatal resistance (β) factor (CLM type); and (lower) rainfall and their interannual differences (mm h^{-1}) from WRF-Chem's baseline simulation. θ is relevant to soil NO and HONO emission modeling and β is a crucial parameter in modeling multiple processes including photosynthesis, photosynthesis-based dry deposition rates, and biogenic isoprene emissions. Rainfall strongly impacts wet deposition modeling and indirectly impacts dry deposition modeling.

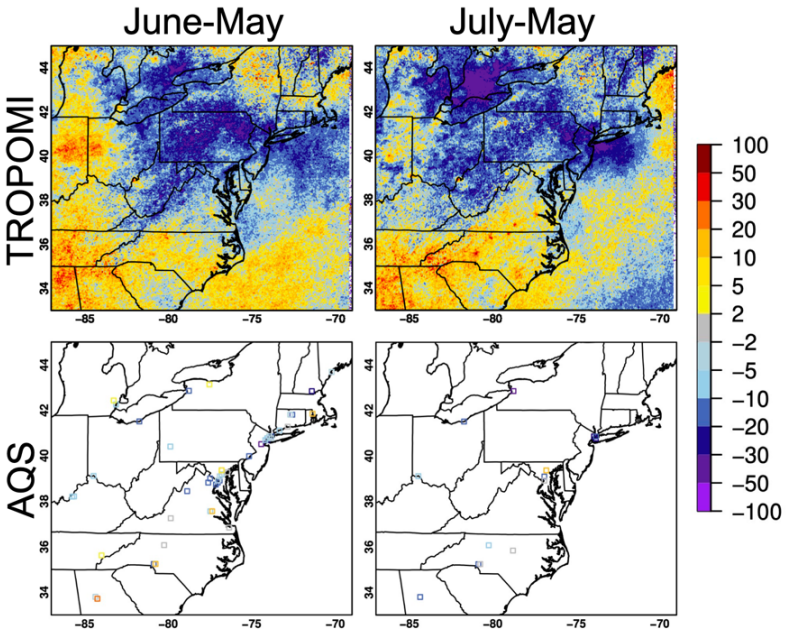

Figure S4: Relative differences (%) of multi-year monthly-mean (upper) TROPOMI NO_2 columns and (lower) AQS 19 UTC surface NO_2 concentrations. Observations from the AQS sites having <10% missing data were used. Note that AQS NO_2 has a strong focus on urban/suburban areas, and as of the last AQS update in October 2023, July 2023 record is less complete than its previous period. WRF-Chem results indicate qualitatively similar spatially-varying (intra)seasonal variability in surface and column NO_2.

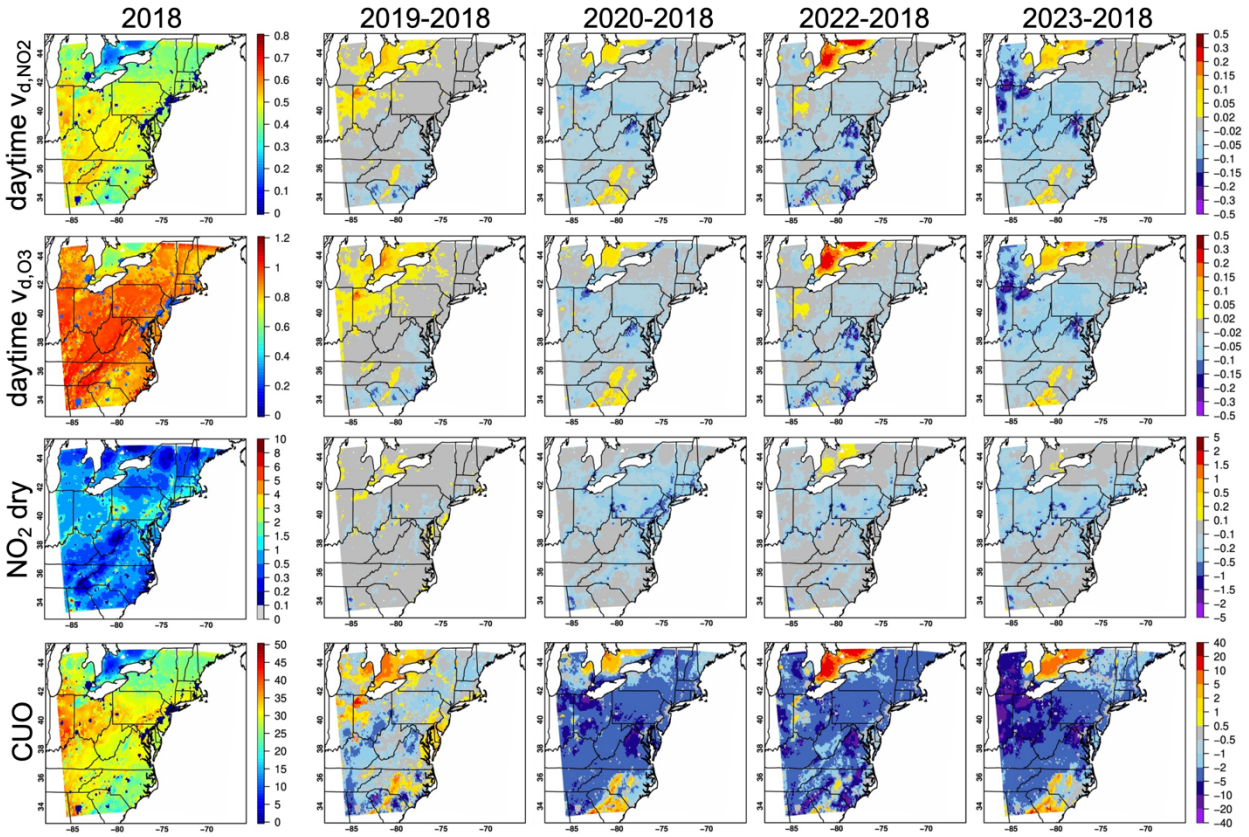

Figure S5: WRF-Chem daytime-average NO_2 and O_3 dry deposition velocities (v_d, cm s^{-1}), as well as NO_2 dry deposition mass fluxes (kgN ha^{-1} a^{-1}) and cumulative O_3 stomatal uptake (mmol m^{-2}). Results are averaged/integrated for MJJ and interannual differences are indicated.

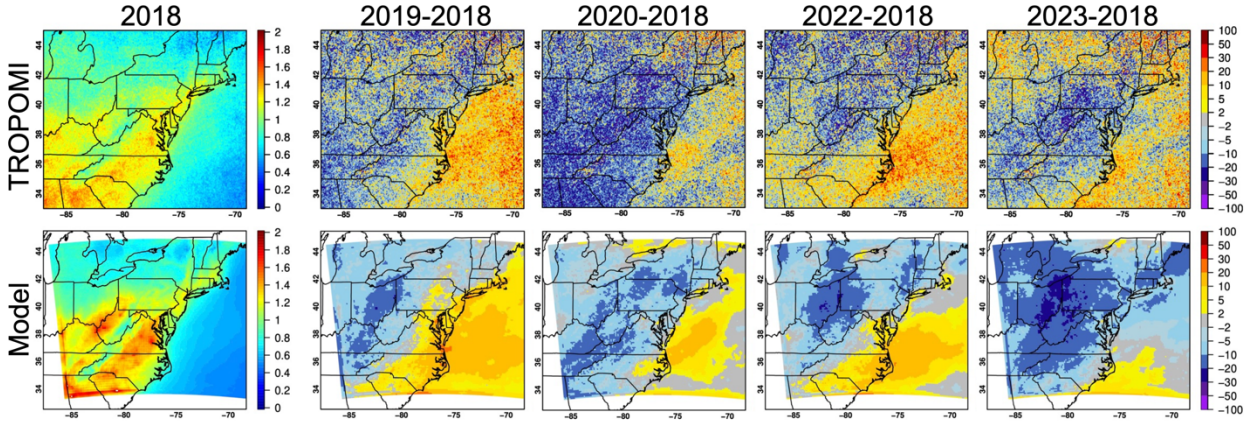

Figure S6: (Upper) TROPOMI and (lower) WRF-Chem HCHO columns. Results are averaged for MJJ 2018 (left, in $\times 10^{16}$ molec. cm^{-2}) and shown together with the % differences between MJJ of each of the following years and 2018.

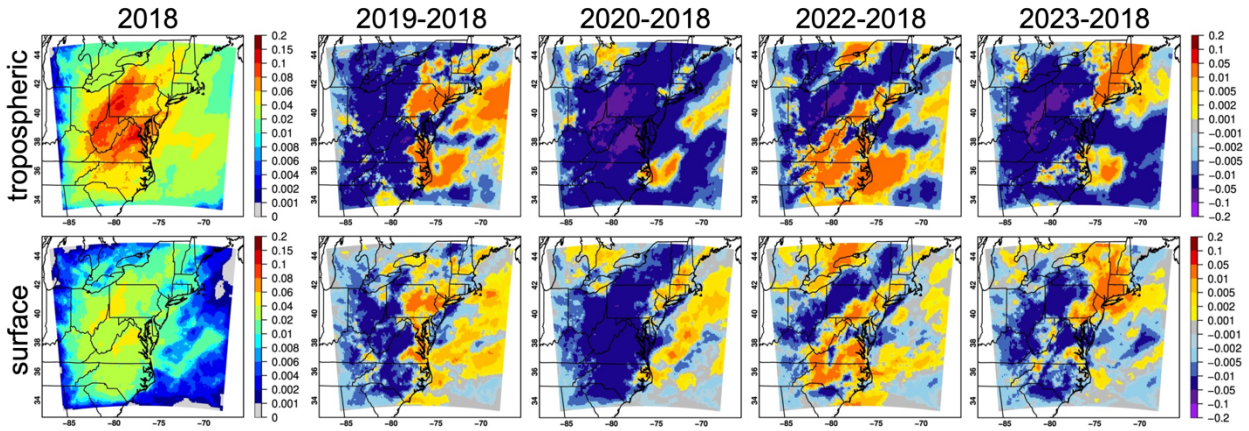

Figure S7: WRF-Chem lightning NO tracer results in ppbv, averaged for 19 UTC of MJJ 2018 and the interannual differences are indicated. Upper and lower panels show tropospheric-column average and surface-level conditions, respectively.

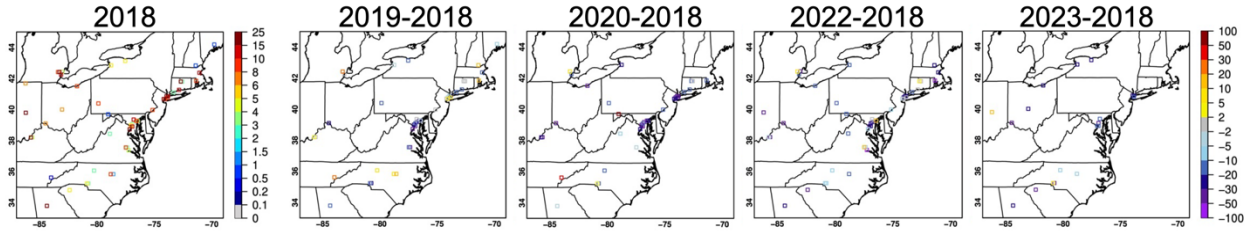

Figure S8: AQS 19 UTC surface NO_2 concentrations. Results are averaged for MJJ 2018 (left, in ppbv), shown together with the % differences between MJJ of each of the following years and 2018. Observations from the AQS sites having <10% missing data for each year were used. Daytime-averaged AQS surface NO_2 indicates qualitatively similar year-to-year changes (not shown).

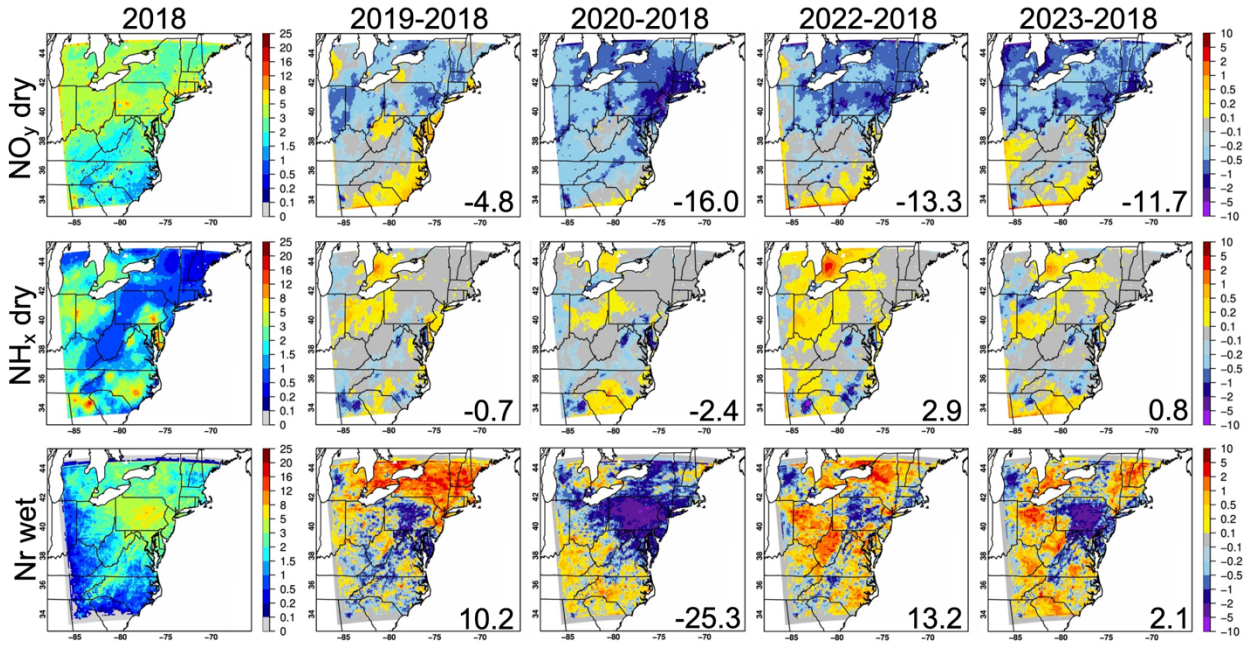

Figure S9: WRF-Chem 2018 MJJ (upper) NO_y dry deposition; (middle) NH_x dry deposition; and (lower) Nr wet deposition fluxes and the differences between MJJ of each of the following years and 2018, all in kgN ha^{-1} a^{-1}. Numbers at the corners of the difference plots indicate the % changes relative to MJJ 2018.

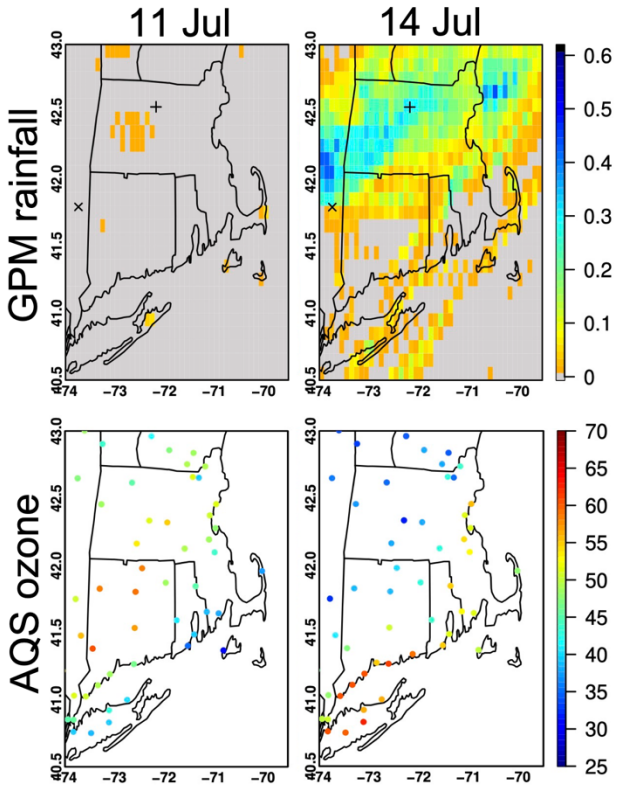

Figure S10: (Upper) GPM/IMERG daily rainfall (mm h^{-1}) on 11 and 14 July 2022. Daily-average rainfall rates measured at the Harvard Forest and the CRN-Millbrook site are both 0 mm h^{-1} on 11 July 2022 and 0.450 and 0.175 mm h^{-1} on 14 July 2022, respectively (data last retrieved from: https://harvardforest1.fas.harvard.edu/exist/apps/datasets/showData.html?id=HF001; and https://www.ncei.noaa.gov/access/crn/sensors.htm?siteId=1118 on 6 February 2024); (lower) AQS surface daytime O_3 observations on 11 and 14 July 2022 for sites having <10% missing data, depicting sharp O_3 decreases in and around Massachusetts soon after the precipitation event occurring ~14 July 2022.

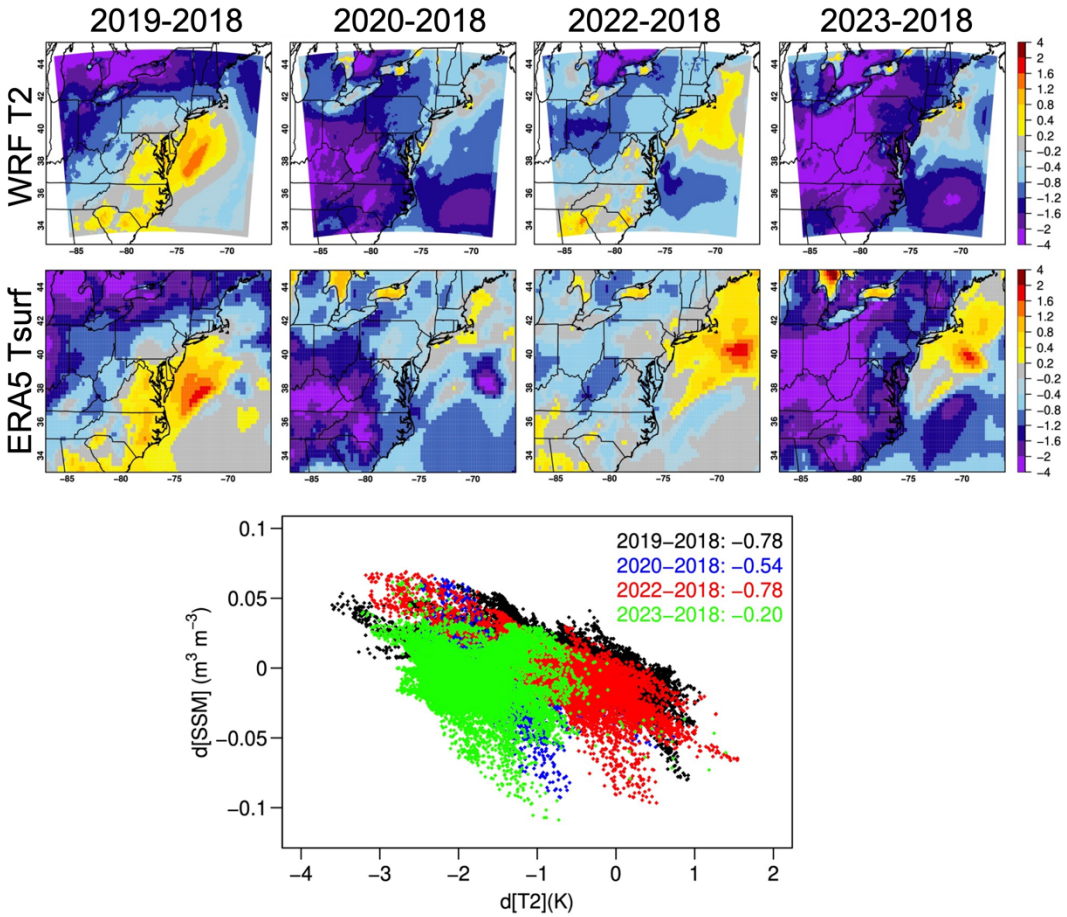

Figure S11: Interannual differences in (upper) WRF daytime 2 m air temperature (T2) and (middle) ERA5 surface air temperature fields in K. The lower panel scatterplot indicates how strong the interannual differences in the modeled surface soil moisture (SSM) influenced the surface air temperature dynamics overland, with their correlation coefficients (p<<0.01) shown in the upper-right legend.

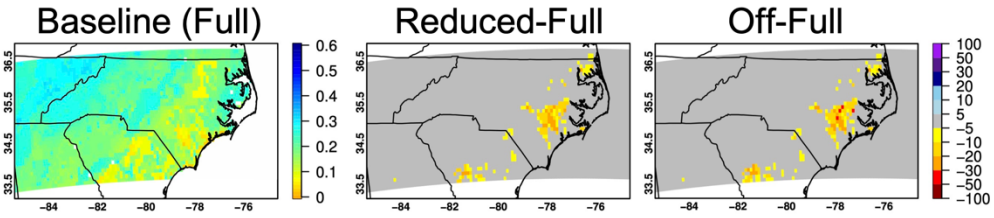

Figure S12: (Left) Noah-MP column-averaged soil moisture (m^3 m^{-3}) over the stressed croplands in the Carolinas, in early mornings of 21–30 June 2022, as well as its % sensitivities to adjustments in irrigation schemes.

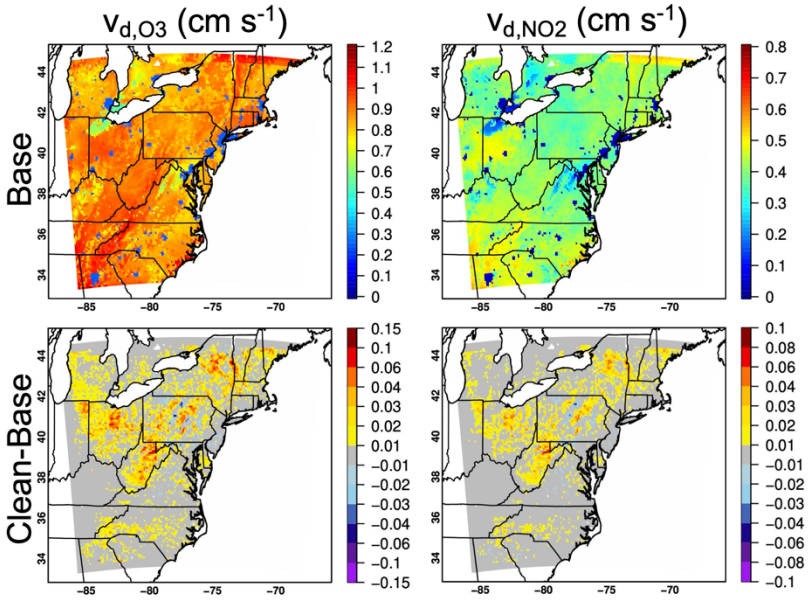

Figure S13: Daytime O_3 and NO_2 dry deposition velocities (cm s^{-1}), averaged for 13–16 June 2023 from the baseline WRF-Chem simulation and their sensitivities to perturbations in chemical boundary conditions.